

- (1995); T. A. Morehead, B. J. Biermann, D. N. Crowell, S. K. Randall, *Plant Physiol.* **109**, 277 (1995); D. Schmitt, K. Callan, W. Gruissem, *ibid.* **112**, 767 (1996).
3. Z. Yang, C. L. Cramer, J. C. Watson, *Plant Physiol.* **101**, 667 (1993); D. Qian, D. Zhou, R. Ju, C. L. Cramer, Z. Yang, *Plant Cell* **8**, 2381 (1996); S. Yalovsky et al., *Mol. Cell. Biol.* **17**, 1986 (1997).
 4. S. Cutler, M. Ghassemian, D. Bonetta, S. Cooney, P. McCourt, *Science* **273**, 1239 (1996).
 5. A. M. Hetherington and R. S. Quatrano, *New Phytol.* **119**, 9 (1991); J. A. D. Zeevaart and R. A. Creelman, *Annu. Rev. Plant Physiol. Plant Mol. Biol.* **39**, 439 (1988); J. Leung and J. Giraudat, *ibid.* **49**, 199 (1998).
 6. S. M. Assmann, *Annu. Rev. Cell Biol.* **9**, 345 (1993); J. M. Ward, Z.-M. Pei, J. I. Schroeder, *Plant Cell* **7**, 833 (1995); E. A. C. MacRobbie, *J. Exp. Bot.* **48**, 515 (1997).
 7. J. I. Schroeder and S. Hagiwara, *Nature* **338**, 427 (1989); R. Hedrich, H. Busch, K. Raschke, *EMBO J.* **9**, 3889 (1990); C. Schmidt, I. Schelle, Y.-J. Liao, J. I. Schroeder, *Proc. Natl. Acad. Sci. U.S.A.* **92**, 9535 (1995); A. Schwartz et al., *Plant Physiol.* **109**, 651 (1995); A. Grabov, J. Leung, J. Giraudat, M. R. Blatt, *Plant J.* **12**, 203 (1997).
 8. Z.-M. Pei, K. Kuchitsu, J. M. Ward, M. Schwarz, J. I. Schroeder, *Plant Cell* **9**, 409 (1997).
 9. D. L. Pompliano et al., *Biochemistry* **31**, 3800 (1992); J. B. Gibbs et al., *J. Biol. Chem.* **268**, 7617 (1993). Guard cell protoplasts (11) or leaves (12) were treated for 2 hours before experiments with 2 μ M HPPA.
 10. J. B. Gibbs and A. Oliff, *Annu. Rev. Pharmacol. Toxicol.* **37**, 143 (1997).
 11. *Arabidopsis thaliana* [Columbia ecotype, *era1-2* (4), *era1/abi1*, and *era1/abi2* (22)] plants were grown in a controlled environment growth chamber with a 16:8 hour light:dark cycle. Guard cell protoplasts were isolated by enzymatic digestion of leaf epidermal strips (8). Whole cell patch-clamp experiments were performed, and data were analyzed as described (8). The solutions used in patch-clamp experiments contained 150 mM CsCl, 2 mM MgCl₂, 6.7 mM EGTA, 3.35 mM CaCl₂, 5 mM tris-GTP, 5 mM Mg-ATP, and 10 mM Hepes-tris (pH 7.1) in the pipette and 30 mM CsCl, 2 mM MgCl₂, 1 mM CaCl₂, and 10 mM MES-tris (pH 5.6) in the bath. For transient K⁺ current ("IAP") recordings, standard solutions were used [Z.-M. Pei, V. M. Baizabal-Aguirre, G. J. Allen, J. I. Schroeder, *Proc. Natl. Acad. Sci. U.S.A.* **95**, 6548 (1998)]. Abscisic acid ([\pm]-*cis,trans*-ABA; Sigma) was freshly added to the bath and pipette solutions. Osmolalities of solutions were adjusted to 485 mmol/kg for bath and 500 mmol/kg for pipette by addition of D-sorbitol. In \approx 30% of guard cells, anion currents did not respond to ABA or HPPA. For unbiased data analysis, nonresponding cells were included in all reported data averages (omission of nonresponding cells would not change conclusions). Statistical analyses were performed with EXCEL (Microsoft). Data are presented as the mean \pm SEM.
 12. Stomatal aperture measurements were conducted as described (8). Detached rosette leaves were floated in solutions containing 20 mM KCl, 1 mM CaCl₂, and 5 mM MES-KOH (pH 6.15) and exposed to light at a fluency rate of 300 μ mol m⁻² s⁻¹. Subsequently, the indicated concentrations of ABA, or 2 μ M HPPA or 5 μ M manumycin, or ABA and 2 μ M HPPA or 5 μ M manumycin were added to the solutions to assay for stomatal closing. After treatments for 2 hours, stomatal apertures were observed with a digital video camera attached to an inverted microscope. Stomatal density was not affected in *era1-2*.
 13. D. F. Zhou, D. Q. Qian, C. L. Cramer, Z. B. Yang, *Plant J.* **12**, 921 (1997).
 14. *ERA1*- β -glucuronidase (GUS) fusion constructs were generated by inserting a 2.5-kb polymerase chain reaction (PCR)-amplified genomic fragment of the *ERA1* promoter into a promoterless GUS T-DNA plasmid (pBI121). This construct was transformed into the *Agrobacterium* strain LB4404. Transgenic plants were generated by vacuum-infiltrating plants with *Agrobacterium* [N. Bechtold, J. Ellis, G. Pelletier, *C. R. Acad. Sci. (Paris)* **316**, 1194 (1993)]. Kanamycin-resistant plants were selected in the next generation, and intact whole leaves were tested for GUS activity with the fluorescent GUS substrate Imagen Green (Molecular Probes, Oregon). Seedlings were incubated in GUS-buffer for 2 to 4 hours at room temperature and then directly viewed under a microscope (magnification, \times 25) by using blue excitation light. Positive fluorescent signal is yellow on a red chlorophyll autofluorescent background.
 15. T. A. Theobald and Z. M. Pei, data not shown (n = 480 stomata in three experiments).
 16. In addition, ABA activation of anion-channel currents was also analyzed at 1 and 50 μ M ABA (n = 23 and 28 cells for WT and *era1-2*, respectively). Activation of anion currents was also potentiated in *era1-2* compared with WT at 1 μ M ABA, whereas at 50 μ M ABA both WT and *era1-2* responses were similar.
 17. M. Koornneef, G. Reuling, C. M. Karssen, *Physiol. Plant.* **61**, 377 (1984); R. R. Finkelstein and C. R. Somerville, *Plant Physiol.* **94**, 1172 (1990).
 18. J. Leung et al., *Science* **264**, 1448 (1994); K. Meyer, M. P. Leube, E. Grill, *ibid.* p. 1452.
 19. J. Leung, S. Merlot, J. Giraudat, *Plant Cell* **9**, 759 (1997).
 20. P. L. Rodriguez, G. Benning, E. Grill, *FEBS Lett.* **421**, 185 (1998).
 21. F. Armstrong et al., *Proc. Natl. Acad. Sci. U.S.A.* **92**, 9520 (1995); J. Sheen, *ibid.* **95**, 975 (1998).
 22. Double mutants of *era1/abi1* and *era1/abi2* were generated by crossing *era1-2* into *abi1-1* and *abi2-1* respectively. F₂ seeds were screened for ABA insensitivity to select for *abi1* or *abi2*. In the next generation seeds were screened for ABA supersensitivity (*era1/era1*). Supersensitive seeds were advanced to the next generation. Homozygous double mutants were identified by PCR amplification with primers of 5'-GATATCTCCGCCGAGAT-3' and 5'-CCATTCCACTGAATCACTTT-3' for *abi1-1*, and 5'-CATCATCTCTGATGGCAGG-3' and 5'-CCGGAGCATGAGCCACAG-3' for *abi2-1*, as described (19). The *era1-2* deletion was verified by Southern (DNA) blot with *ERA1* cDNA as a probe. The *era1/abi1* mutant was further verified by back crosses to both parents to confirm genetically that it was a double mutant.
 23. M. R. G. Roelfsema and H. B. A. Prins, *Physiol. Plant.* **95**, 373 (1995).
 24. C. M. Kwak, data not shown (n = 960 stomata for *era1/abi1* experiments; n = 220 stomata for drought experiments).
 25. C. M. Kwak, data not shown. ABA inhibition of seed germination was analyzed as described (17). Germination of seeds was defined as positive when a radical tip had fully penetrated the seed coat (n = 50 per condition). Each experiment (n = 25) included conditions comparing the indicated lines at multiple ABA concentrations.
 26. Transpiration rate and soil moisture were measured as described [N. Vartanian, L. Marcotte, J. Giraudat, *Plant Physiol.* **104**, 761 (1994)]. For drought experiments, seeds of both WT (Col) and *era1-2* were germinated in individual pots each containing the same amount of prewetted soil. Plants were grown under constant light (200 μ mol m⁻² s⁻¹) and watered by irrigation until just before the plants bolted (\approx 3 weeks). Because *era1* affects growth, WT and *era1-2* plants (n = 16 each) were selected that were at the same developmental stages and had similar numbers of leaves. At this point pots were removed from water and allowed to dry over time. Evaporation from soil was reduced by covering the soil surface with tinfoil so that water loss occurring primarily through plant transpiration could be quantified. Watered control plants were also analyzed. Pots were weighed every day at the same time. Pots containing no plants were subjected to the same treatments to determine the background rate of water loss.
 27. P. McCourt, unpublished data.
 28. W. R. Schafer et al., *Science* **245**, 379 (1989); J. F. Hancock, A. I. Magee, J. E. Childs, C. J. Marshall, *Cell* **57**, 1167 (1989); R. E. Barrington et al., *Mol. Cell. Biol.* **18**, 85 (1998); M. M. Moasser et al., *Proc. Natl. Acad. Sci. U.S.A.* **95**, 1369 (1998).
 29. J. K. Zhu, R. A. Bressan, P. M. Hasegawa, *Proc. Natl. Acad. Sci. U.S.A.* **90**, 8557 (1993).
 30. We thank T. A. Theobald, V. M. Baizabal-Aguirre, K. Kuchitsu, and X.-F. Cheng for assistance, and E. J. Kim, G. J. Allen, W. R. Schafer, N. M. Crawford, M. F. Yanofsky, and R. Y. Hampton for discussions and reading of the manuscript. Supported by National Science Foundation (MCB-9506191) and Department of Energy grants (94-ER20148) to J.I.S. and by a Natural Science and Engineering Research Council of Canada grant to P.M.

29 April 1998; accepted 10 August 1998

Cell Surface Trafficking of Fas: A Rapid Mechanism of p53-Mediated Apoptosis

Martin Bennett,* Kirsty Macdonald, Shiu-Wan Chan, J. Paul Luzio, Robert Simari, Peter Weissberg

p53 acts as a tumor suppressor by inducing both growth arrest and apoptosis. p53-induced apoptosis can occur without new RNA synthesis through an unknown mechanism. In human vascular smooth muscle cells, p53 activation transiently increased surface Fas (CD95) expression by transport from the Golgi complex. Golgi disruption blocked both p53-induced surface Fas expression and apoptosis. p53 also induced Fas-FADD binding and transiently sensitized cells to Fas-induced apoptosis. In contrast, *lpr* and *gld* fibroblasts were resistant to p53-induced apoptosis. Thus, p53 can mediate apoptosis through Fas transport from cytoplasmic stores.

p53 is the most commonly mutated gene in human cancer (1). p53 is a sequence-specific transcription factor, whose transcriptional targets induce growth arrest and apoptosis (2). Although its tumor suppressor function requires both activities, some human tumor-derived p53 mutants transactivate p53-responsive promoters and induce growth arrest, implying that apoptosis is the more potent

mechanism (3). Depending on cell type, p53-induced apoptosis either requires transcriptional activation (4) or occurs without new RNA and protein synthesis (5). The occurrence of mutants that transactivate p53 targets but are defective for apoptosis (6), or vice versa (7), suggests that p53 induces apoptosis through transactivation-dependent and -independent mechanisms, implying a structural

REPORTS

and functional separation between the ability to induce growth arrest or apoptosis.

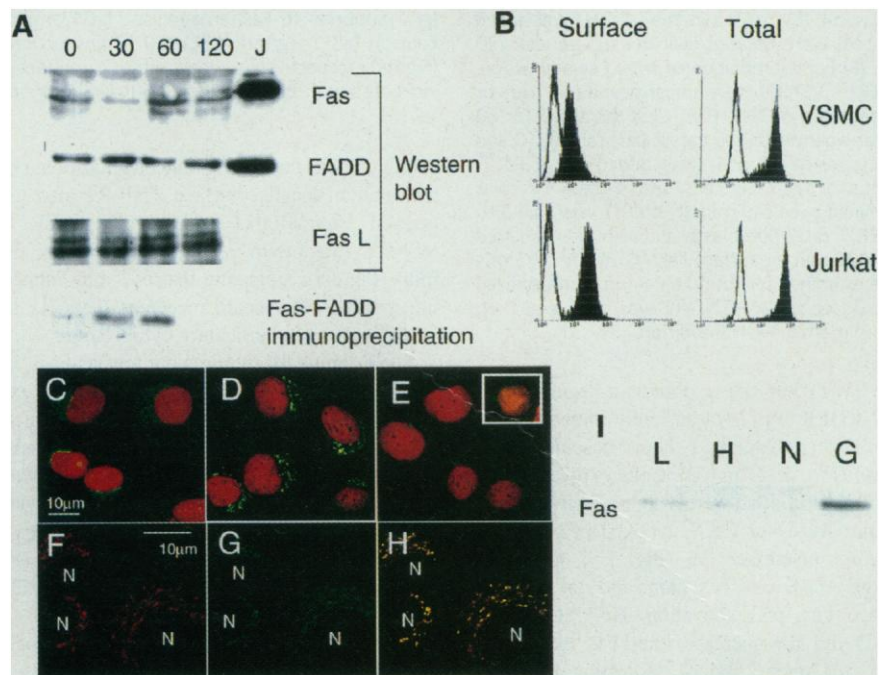
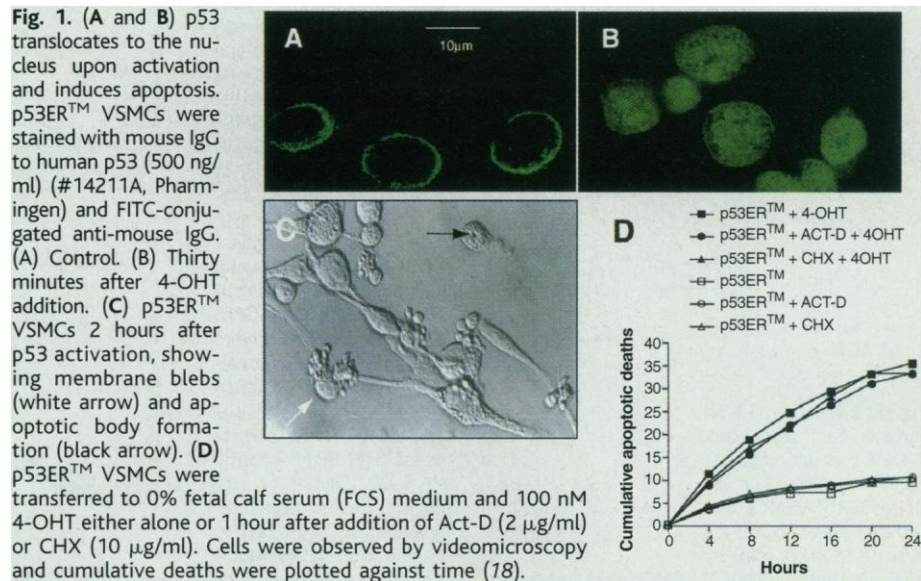
We examined p53-mediated apoptosis in untransformed human vascular smooth muscle cells (VSMCs) by expressing a conditional allele of p53, p53ERTM (8), encoding a chimeric full-length human p53 fused to a 4-hydroxytamoxifen (4-OHT)-sensitive estrogen receptor (9). 4-OHT addition to p53ERTM VSMCs rapidly activates p53 (10), caused translocation of perinuclear p53 to the nucleus (Fig. 1, A and B), and induced apoptosis (Fig. 1C), with apoptotic morphology first appearing within 60 min. Apoptosis was not inhibited by preincubation with actinomycin D (Act-D) or cycloheximide (CHX) at concentrations that completely block RNA or protein synthesis (10) (Fig. 1D). Neither Act-D nor CHX alone induced apoptosis (Fig. 1D), indicating that apoptosis of p53ERTM VSMCs was transcription-independent.

Apoptosis through Fas (CD95), a tumor necrosis factor receptor (TNF-R) family member, is rapid and independent of new RNA or protein synthesis (11). Fas ligand (FasL)-Fas binding recruits an adapter molecule, FADD, through shared protein motifs ("death domains"), with resultant caspase activation leading to apoptosis. We therefore analyzed Fas, FADD, and FasL expression and Fas-FADD binding after p53 activation. No increases in Fas, FADD, or FasL protein were observed (Fig. 2A). However, FADD coimmunoprecipitated with Fas 30 to 60 min after p53 activation, but Fas-FADD binding disappeared by 2 hours.

We next examined both surface and total Fas expression in VSMCs. VSMCs expressed little surface Fas, compared with Jurkat cells (Fig. 2B), but total Fas (in permeabilized cells) was much greater than surface expression, indicating that Fas was predominantly intracellular (12). Fas immunocytochemistry demonstrated a compact, perinuclear distribution that colocalized with the Golgi marker galactosyl transferase (Fig. 2, C to H). Brefeldin A (BFA), a protein-secretion inhibitor that redistributes Golgi proteins to the endoplasmic reticulum (ER) or near the microtubular organizing center (13), disrupted Fas staining to produce an ER-like pattern (Fig. 2E), with fluorescent spots abutting the nucleus (Fig. 2E, inset). Thus, Fas localized to the Golgi complex and trans-Golgi

network. Subfractionation of VSMC homogenates and protein immunoblotting confirmed Fas in the Golgi-enriched fraction (Fig. 2I).

To examine p53 regulation of Fas distribution, we measured surface Fas by flow cytometry after p53 activation. Activation of wild-



M. Bennett, K. Macdonald, S.-W. Chan, P. Weissberg, Department of Medicine, University of Cambridge, Addenbrooke's Hospital, Cambridge CB2 2QQ, UK. J. P. Luzio, Department of Clinical Biochemistry, University of Cambridge, Addenbrooke's Hospital, Cambridge CB2 2QQ, UK. R. Simari, Department of Cardiovascular Diseases, Biochemistry and Molecular Biology, Mayo Clinic and Foundation, Rochester, MN 55905, USA.

*To whom correspondence should be addressed. E-mail: mrb@mole.bio.cam.ac.uk

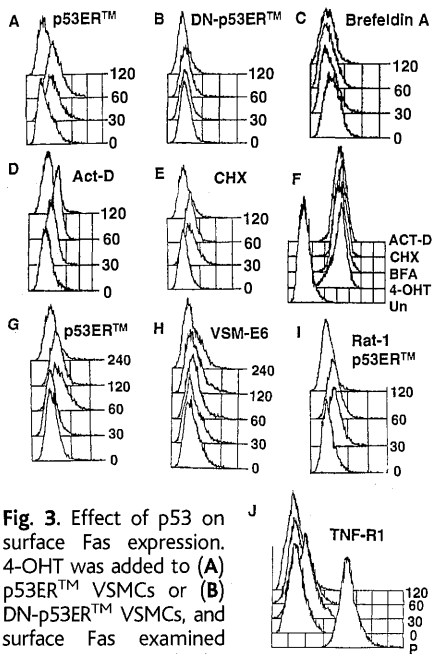


Fig. 3. Effect of p53 on surface Fas expression. 4-OHT was added to (A) p53ERTM VSMCs or (B) DN-p53ERTM VSMCs, and surface Fas examined over 0 to 120 min by flow cytometry. p53ERTM VSMCs were incubated in BFA (5 μg/ml) (C), Act-D (2 μg/ml) (D), or CHX (10 μg/ml) (E) for 60 min, then 4-OHT was added and cells were isolated over the subsequent 120 min. (F) For examination of total Fas expression, p53ERTM VSMCs were unpermeabilized (Un) or treated with 4-OHT, BFA, CHX, or Act-D for 60 min and permeabilized before Fas staining. (G and H) Etoposide (5 μM) was added to p53ERTM VSMCs or VSM-E6 cells and surface Fas was examined over 240 min. (I) 4-OHT was added to p53ERTM rat 1 fibroblasts, and cells were isolated over 120 min for surface Fas. (J) p53ERTM VSMCs were examined for total TNF-R1 in permeabilized cells (P) or surface TNF-R1 was examined 0 to 120 min after 4-OHT addition.

type (WT) but not a dominant-negative p53 (DN-p53ERTM) (14) transiently increased surface Fas (maximum 1 hour, baseline by 2 hours) (Fig. 3, A and B). Cells expressing the ERTM vector alone were also ineffective. BFA, but not Act-D or CHX, blocked p53-induced increases in surface Fas (Fig. 3, C to E), although Act-D or CHX alone did not increase surface Fas. p53 activation, BFA, CHX, or Act-D did not increase total Fas expression (Fig. 3F) over 2 hours, indicating that p53 caused cell surface redistribution of cytoplasmic Fas.

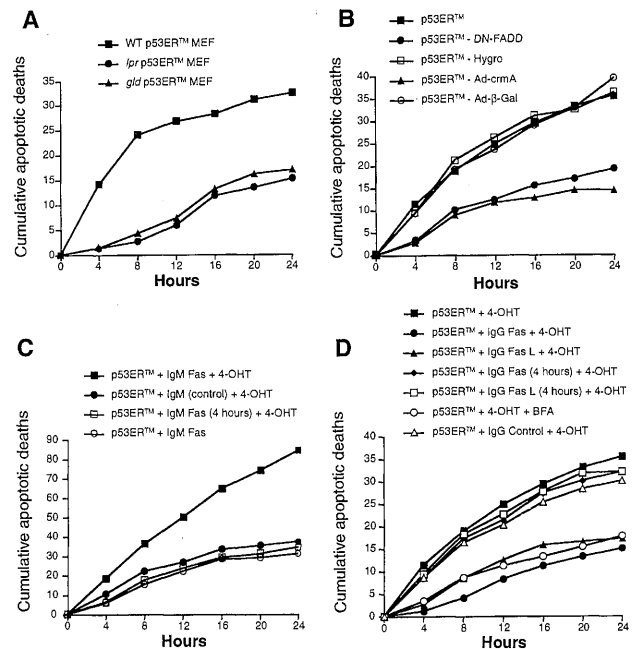
To determine whether p53 that was induced after DNA damage increased surface Fas, we treated p53ERTM cells or VSMCs expressing human papilloma virus E6 [which lacks functional p53 (10)] (VSM-E6 cells) with the topoisomerase II inhibitor etoposide. Etoposide transiently increased surface Fas in p53ERTM but not VSM-E6 cells (Fig. 3, G and H), albeit delayed (maximum 2 hours, baseline by 4 hours) compared with 4-OHT activation. 4-OHT activation of p53ERTM in rat 1 fibroblasts (Fig. 3I) and WT mouse embryo fibroblasts (MEFs) also increased surface Fas, indi-

Fig. 4. p53-induced apoptosis requires Fas and FasL. (A) Wild-type, *lpr*, and *gld* MEFs were transiently infected with p53ERTM, cells were transferred to medium containing 0% FCS and 4-OHT, and apoptosis was observed by videomicroscopy. (B) p53ERTM VSMCs stably expressing DN-FADD or vector (Hygro) (21), or cells infected with an adenovirus encoding *crmA* (Ad-*crmA*) (22) or β-galactosidase (Ad-β-Gal) were transferred to medium containing 0% FCS and 4-OHT. (C) p53ERTM VSMCs were incubated in 0% FCS medium. An agonistic IgM antibody to Fas (CH-11) or isotypically matched control mouse IgM (IgM control; #M-5909, Sigma) (1 μg/ml) was added either simultaneously (IgM Fas) or 4 hours after 4-OHT addition [IgM Fas (4 hours)]. In addition, p53ERTM VSMCs were incubated with CH-11 but without 4-OHT. (D) p53ERTM VSMCs were incubated in medium containing 0% FCS and 4-OHT and an antagonistic IgG1 antibody to Fas, antagonistic IgG1 antibody to FasL, or isotypically matched mouse IgG (IgG control) (all 1 μg/ml) [#F22120 (Transduction Labs), NOK-1 (#65320C, Pharmingen), and M-5284 (Sigma), respectively] added either simultaneously or 4 hours later. p53ERTM VSMCs were also incubated with BFA (5 μg/ml) 60 min before transfer to 0% FCS medium and 4-OHT.

cating that Fas trafficking may be widespread in mesenchymal cells. Surface TNF-R1 also increased after 4-OHT addition to p53ERTM VSMCs (maximum 30 min, baseline by 60 min) (Fig. 3J), indicating that p53 may induce transport of other death receptors. TNF-R1 in VSMCs was predominantly cytoplasmic.

To examine the requirement for Fas-FasL in early p53-induced apoptosis, we transiently expressed p53ERTM in *lpr* or *gld* MEFs, which contain inactivating mutations in Fas and FasL, respectively (15). p53-induced apoptosis was reduced in *lpr* and *gld* MEFs compared with WT (Fig. 4A). In addition, a dominant-negative (DN) FADD or *crmA*, which both inhibit Fas-mediated apoptosis (16, 17), also inhibited p53-mediated apoptosis (Fig. 4B).

To confirm that Fas transported after p53 activation could induce apoptosis, we incubated p53ERTM VSMCs with an agonistic immunoglobulin M (IgM) antibody to Fas (anti-Fas) (CH-11) or control antibody. CH-11 increased apoptosis only after p53 activation, although this effect disappeared if addition was delayed 4 hours after p53 activation (Fig. 4C). CH-11 did not induce apoptosis in ERTM or DN-p53ERTM cells. Consistent with these findings, neutralizing anti-Fas or FasL antibodies inhibited apoptosis of p53ERTM VSMCs only if added <4 hours after p53 activation (Fig. 4D), indicating that Fas-FasL death signals are completed within 4 hours of p53 activation. BFA inhibited apoptosis in low-serum medium only after p53 activation (Fig. 4D), further confirming that



early p53-induced apoptosis of VSMCs requires surface transport of Fas.

p53-induced apoptosis clearly involves several mechanisms, with transcription-dependent or -independent pathways being determined by cell type and apoptotic stimulus. However, we have found that p53 activation can regulate sensitivity to apoptosis by allowing cytoplasmic death receptors to redistribute to the cell surface. Tumor cells lacking functional p53 will evade apoptosis induced by both p53 transcriptional targets and FasL. Intracellular sequestration of death receptors may cause resistance to apoptosis and insensitivity to chemotherapeutic agents for cancer. Conversely, therapy based on cell surface redistribution of death receptors may promote apoptosis through endogenous ligands.

References and Notes

1. M. Hollstein et al., *Nucleic Acids Res.* **22**, 3551 (1994).
2. W. S. el Deiry et al., *Cell* **75**, 817 (1993); M. Kastan et al., *ibid.* **71**, 587 (1992); L. Buckbinder et al., *Nature* **377**, 646 (1995); T. Miyashita et al., *Oncogene* **9**, 1799 (1994); D. Israeli et al., *EMBO J.* **16**, 4384 (1997); K. Polyak, Y. Xia, J. L. Zweier, K. W. Kinzler, B. Vogelstein, *Nature* **389**, 300 (1997).
3. K. Ory, Y. Legros, C. Auguin, T. Soussi, *EMBO J.* **13**, 3496 (1994).
4. E. Yonish-Rouach et al., *Oncogene* **11**, 2197 (1995); L. Donatella Attardi, S. Lowe, J. Brugarolas, T. Jacks, *EMBO J.* **15**, 3693 (1996); P. Sabbatini, J. Lin, A. Levine, E. White, *Genes Dev.* **9**, 2184 (1995).
5. C. Caelles, A. Helmberg, M. Karin, *Nature* **370**, 220 (1994); A. J. Wagner, J. M. Kokontis, N. Hay, *Genes Dev.* **8**, 2817 (1994).
6. S. Rowan et al., *EMBO J.* **15**, 827 (1996).

7. Y. Haupt, S. Rowan, E. Shaulian, K. Vousden, M. Oren, *Genes Dev.* **9**, 2170 (1995); C. Ishioka *et al.*, *Oncogene* **10**, 1485 (1995).
8. pBabepuro p53ERTM or DN-p53ERTM was transfected into PA317 retroviral packaging cells. Recombinant retrovirus harvested at 48 hours was used to infect VSMCs, rat 1 fibroblasts, or MEFs in polybrene (8 µg/ml). Cells were selected in puromycin (2.5 µg/ml) and resistant cells were pooled.
9. T. Littlewood, D. Hancock, P. Danielian, M. Parker, G. Evan, *Nucleic Acids Res.* **23**, 1686 (1995).
10. M. Bennett, T. Littlewood, S. Schwartz, P. Weissberg, *Circ. Res.* **81**, 591 (1997).
11. S. Yonehara, A. Ishii, M. Yonehara, *J. Exp. Med.* **169**, 1747 (1989); N. Itoh *et al.*, *Cell* **66**, 233 (1991).
12. Cells (1×10^6) were incubated with CH-11 (20 µg/ml) for 30 min on ice followed by a secondary fluorescein isothiocyanate-conjugated anti-mouse IgG (Sigma). Total Fas expression was analyzed by permeabilizing cells in ethanol for 30 min before Fas staining. Higher expression of cytoplasmic compared with surface Fas was evident in rat and human fibroblasts, mesangial cells, and rat VSMCs, but not in THP-1 or HeLa cells.
13. R. Klausner, J. Donaldson, J. Lippincott-Schwartz, *J. Cell Biol.* **116**, 1071 (1992); M. Ladinsky and K. Howell, *Eur. J. Cell Biol.* **59**, 92 (1992).
14. DN-p53(302-370) encodes the oligomerization domain of p53 [E. Shaulian, A. Zauberman, D. Ginsberg, M. Oren, *Mol. Cell Biol.* **12**, 5581 (1992)].
15. R. Watanabe-Fukunaga, C. I. Brannan, N. G. Copeland, N. A. Jenkins, S. Nagata, *Nature* **356**, 314 (1992); T. Takahashi *et al.*, *Cell* **76**, 969 (1994).
16. A. Chinnaiyan, K. O'Rourke, M. Tewari, V. Dixit, *Cell* **81**, 505 (1995). DN-FADD [(FADD(80-208)] contains the death domain of FADD and therefore binds Fas, but lacks the NH₂-terminal death effector domain required for apoptosis.
17. C. A. Ray *et al.*, *Cell* **69**, 597 (1992); M. Tewari and V. Dixit, *J. Biol. Chem.* **270**, 597 (1995); K. Smith, A. Strasser, D. Vaux, *EMBO J.* **15**, 5167 (1996).
18. Time-lapse videomicroscopy examined the course of 100 randomly selected cells over 24 hours. Cumulative apoptotic deaths at 4-hour intervals were plotted against time. Mean deaths for each time point and experimental condition for a minimum of three independent experiments are given. Videomicroscopic measurements of apoptosis were confirmed against trypan blue exclusion (a measure of loss of viability).
19. Mouse anti-Fas IgG (10 µg/ml) was bound to protein G-Sepharose (1 hour, 4°C). p53ERTM VSMC lysates were incubated with anti-Fas-protein G complexes (3 hours, 4°C), precipitated, separated by 10% SDS-polyacrylamide gel electrophoresis (PAGE) in non-reducing conditions, and blotted with mouse anti-human FADD IgG (1 µg/ml).
20. p53ERTM VSMCs (5×10^6) were incubated in nocodazole (10 µg/ml) and latrunculin A (5 µg/ml) in 10 mM Hepes (pH 7.4) for 30 min at 37°C. The cell sediment was first swollen with 150 mM KCl, 10 mM tris-acetate-EDTA (pH 7.4) for 10 min on ice, washed twice in KEHM [150 mM KCl, 10 mM EGTA, 50 mM Hepes-KOH (pH 7.4), 2 mM MgCl₂], and protease inhibitor cocktail (PIC, Sigma), resuspended in an equal volume of KEHM, and homogenized. The homogenate was centrifuged through a discontinuous sucrose gradient (1.6, 1.2, or 0.8 M sucrose in KEHM and PIC), and the Golgi-enriched fraction was collected from the 0.8/1.2 M sucrose interface, separated by 10% SDS-PAGE, blotted, and probed with mouse anti-Fas IgG (100 ng/ml) (#F22120, Transduction Labs). Fractions were compared against homogenate, and whole-cell lysate was isolated for protein immunoblots.
21. Retroviruses encoding pBabe Hygro FADD-DN or control vector (pBabe Hygro) [A. O. Hueber *et al.*, *Science* **278**, 1305 (1997)] were synthesized as in (10), cells were selected in hygromycin (200 µg/ml), and resistant cells were pooled.
22. A Nru-Dra III fragment from pcDNA3 crmA (16), cloned into the adenovirus shuttle plasmid pAdBglII, was cotransfected with Xba I-Cla I-digested sub360 genomic DNA [T. Ohno *et al.*, *Science* **265**, 781 (1994)] into 293 cells. Recombinant virus was isolated by plaque purification, propagated in 293 cells,

and purified by caesium chloride centrifugation. Virus titers were determined by plaque assay. Target cell infection of 100% was obtained with a multiplicity of infection of 100 per cell.

23. We thank R. Hicks for flow cytometry, T. Littlewood for pBabe p53ERTM, E. Nabel and G. Nabel for crmA adenovirus, D. Galloway for pLHPV-E6 type 16, A. Hueber for *lpr* and *gld* MEFs and pBabe DN-FADD, T. Suganuma for anti-galactosyl transferase, and F.

Buss, G. Evan, and M. Oren for advice and comments. Supported by British Heart Foundation grants FS/97024, PG/95057, and PG/96040 (to M.B.) and CH/9400 (to P. W.), Medical Research Council grant G9310915 (to J.P.L.), and NIH grant HL34073 and the Bruce and Ruth Rappaport Program in Vascular Biology (to R.S.).

7 April 1998; accepted 4 September 1998

Bifurcation of Lipid and Protein Kinase Signals of PI3K γ to the Protein Kinases PKB and MAPK

Tzvetanka Bondeva,* Luciano Pirola,* Ginette Bulgarelli-Leva, Ignacio Rubio, Reinhard Wetzker, Matthias P. Wymann†

Phosphoinositide 3-kinases (PI3Ks) activate protein kinase PKB (also termed Akt), and PI3K γ activated by heterotrimeric guanosine triphosphate-binding protein can stimulate mitogen-activated protein kinase (MAPK). Exchange of a putative lipid substrate-binding site generated PI3K γ proteins with altered or aborted lipid but retained protein kinase activity. Transiently expressed, PI3K γ hybrids exhibited wortmannin-sensitive activation of MAPK, whereas a catalytically inactive PI3K γ did not. Membrane-targeted PI3K γ constitutively produced phosphatidylinositol 3,4,5-trisphosphate and activated PKB but not MAPK. Moreover, stimulation of MAPK in response to lysophosphatidic acid was blocked by catalytically inactive PI3K γ but not by hybrid PI3K γ s. Thus, two major signals emerge from PI3K γ : phosphoinositides that target PKB and protein phosphorylation that activates MAPK.

PI3Ks play a central role in cell signaling and lead to cell proliferation and survival, motility, secretion, and specialized cell responses such as the respiratory burst of granulocytes (1). It is assumed that these responses are mediated by the major lipid product of the class I PI3K family, phosphatidylinositol 3,4,5-trisphosphate [PtdIns(3,4,5)P₃]. The protein kinase PKB is a direct target of PtdIns(3,4)P₂ (2) and is further activated by phosphoinositide-dependent kinases (PDKs) (3).

Heterodimeric p85/p110 PI3K α and PI3K γ both have protein kinase activity (4, 5). Moreover, PI3K α -mediated phosphorylation of its regulatory p85 subunit decreases the enzyme's lipid kinase activity (4). The functions of PI3K have often been established with the PI3K inhibitors wortmannin and LY294002 or with catalytically inactive PI3K constructs (6, 7). Such manipulations interfere with both lipid and protein kinase activities of PI3Ks (4, 5), and a physiological role of PI3K signaling

through its protein kinase activity has not been established. We therefore engineered PI3Ks that allowed us to separately study the lipid and protein kinase activities of PI3K γ .

A region within the conserved catalytic core of PI3K γ (8) was replaced by the corresponding sequences of PI3Ks of class II (which phosphorylate PtdIns or PtdIns 4-*P* in vitro), class III (restricted to PtdIns), and FRAP [a member of the target of rapamycin family without assigned lipid kinase activity (Fig. 1A)]. The exchanged sequences correspond to the activation loop in cAMP-dependent protein kinase and insulin receptor tyrosine kinase and seem to regulate the access of PI substrates to the catalytic core (9). When expressed in 293 cells as glutathione-S transferase (GST)-PI3K γ fusion proteins, purified wild-type PI3K γ phosphorylated PtdIns, PtdIns 4-*P*, and PtdIns(4,5)P₂, whereas the hybrid of PI3K γ with a class II insert (cII) phosphorylated only PtdIns and PtdIns 4-*P* (Fig. 1B). In vitro production of PtdIns 3-*P* by cII was equal to that of the wild-type enzyme (1.1-fold, ± 0.1 SE, $n = 3$) in the absence of cholate and much greater than that of wild type in the presence of cholate (22.9-fold, ± 2.7 SE, $n = 5$). The hybrid with a class III insert (cIII) behaved like the PtdIns 3-kinase involved in vacuolar protein sorting (Vps34p) and

T. Bondeva, I. Rubio, R. Wetzker, Research Unit "Molecular Cell Biology," University of Jena, D-07747 Jena, Germany. L. Pirola, G. Bulgarelli-Leva, M. P. Wymann, Institute of Biochemistry, University of Fribourg, CH-1700 Fribourg, Switzerland.

*These authors contributed equally to this work.

†To whom correspondence should be addressed. E-mail: Matthias.Paul.Wymann@Unifr.ch